Inorganic Chemistry

Article

pubs.acs.org/IC

Photocatalytic Reduction of Artificial and Natural Nucleotide Co-factors with a Chlorophyll-Like Tin-Dihydroporphyrin Sensitizer

Kerstin T. Oppelt,[†] Eva Wöß,[†] Martin Stiftinger,[‡] Wolfgang Schöfberger,[†] Wolfgang Buchberger,[‡] and Günther Knör*,[†]

[†]Institute of Inorganic Chemistry, and [‡]Institute of Analytical Chemistry, Johannes Kepler University Linz (JKU), A-4040 Linz, Austria

Supporting Information

ABSTRACT: An efficient photocatalytic two-electron reduction and protonation of nicotine amide adenine dinucleotide (NAD^+), as well as the synthetic nucleotide co-factor analogue *N*-benzyl-3-carbamoyl-pyridinium ($BNAD^+$), powered by photons in the long-wavelength region of visible light (λ_{irr} > 610 nm), is demonstrated for the first time. This functional artificial photosynthetic counterpart of the complete energy-trapping and solar-to-fuel conversion primary processes occurring in natural photosystem I (PS I) is achieved with a robust water-soluble tin(IV) complex of *meso*-tetrakis(*N*-methylpyridinium)-chlorin acting as the light-harvesting sensitizer (threshold wavelength of λ_{thr} = 660 nm). In buffered aqueous solution, this chlorophyll-like compound photocatalytically recycles a rhodium hydride complex of the type $[Cp^*Rh(bpy)H]^+$, which is able to mediate regioselective hydride transfer processes. Different one- and two-electron donors are tested for the reductive quenching of the irradiated tin complex to initiate the secondary dark reactions leading to nucleotide co-factor reduction. Very promising conversion efficiencies, quantum yields, and excellent photosensitizer stabilities are observed. As an example of a catalytic dark reaction utilizing the reduction equivalents of accumulated NADH, an enzymatic process for the selective transformation of aldehydes with alcohol dehydrogenase (ADH) coupled to the primary photoreactions of the system is also demonstrated. A tentative reaction mechanism for the transfer of two electrons and one proton from the reductively quenched tin chlorin sensitizer to the rhodium co-catalyst, acting as a reversible hydride carrier, is proposed.

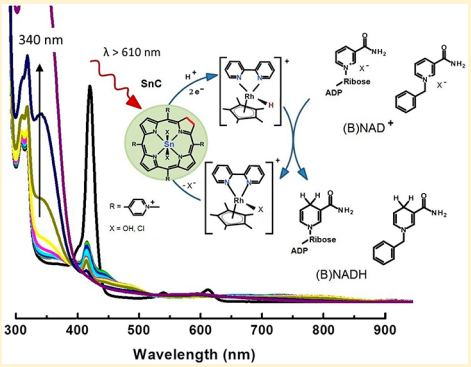

1. INTRODUCTION

Protonated nicotine amide adenine dinucleotide (NADH) produced in the course of photosynthetic energy conversion can be considered as the biological equivalent of solar hydrogen as a fuel.[1] As a versatile two-electron reductant, this co-factor is an essential component for many biocatalytic and bioinspired substrate transformation processes, requiring competent electron input for chemical bond formation.[2−4] For example, the assimilation of atmospheric CO_2 to produce liquid carbon-based fuels such as methanol can be achieved via an enzymatic reduction sequence based on NADH.[5] A variety of biomimetic asymmetric hydrogenation reactions also critically depends on the availability of this class of redox co-factors.[6,7] For many of these potential applications, however, a permanent addition of the native co-factor as a sacrificial reductant remains costly and impractical. Therefore, a sustainable recycling method for nicotine amide adenine dinucleotide (NAD^+) and related model compounds based on a renewable energy source is a highly desirable feature.[8−11] Here, we report about the efficient nonenzymatic regeneration of native NADH and the functional nucleotide co-factor analogue BNADH (protonated *N*-benzyl-3-carbamoyl-pyridinium) powered by red light, using a water-soluble tin(IV)chlorin complex as a novel chlorophyll-like photosensitizer for solar chemistry.

Because of their excellent stability properties and a preference for mediating multielectron transfer processes,[12−14] tin porphyrins are very attractive candidates for the sensitization of artificial photosynthetic reactions based on earth-abundant components. Some of their water-soluble derivatives have been successfully involved in pioneering studies on the photogeneration of hydrogen under visible-light irradiation.[15,16] The photochemical formation of different aromatic ring-reduced hydroporphyrin species is a common observation under these conditions.[17,18] In this context, the occurrence of tin chlorins (SnC), which are stable 2,3-dihydroporphyrin derivatives of their porphyrin parent compounds (SnP), has been considered as an undesirable side reaction, which could no longer be coupled to hydrogen production.[15,19] In combination with a suitable hydride transfer mediator, however, the chlorin species SnC, which exhibits attractive chlorophyll-type spectral features, including an enhanced red light-absorption capability, becomes accessible as a photocatalyst for the accumulation and transfer of hydrogen equivalents. This novel approach allows the harvesting of low-energy photons for a more efficient solar energy

Received: June 25, 2013
Published: September 27, 2013

Scheme 1. Photochemical Reduction of Water-Soluble Tin Porphyrin Complexes (SnP) To Generate the Two-Electron Reduced Tin(IV)-*meso*-tetrakis(*N*-methylpyridinium)chlorin Derivatives (SnC) upon Green Light Irradiation under Aerobic Conditions

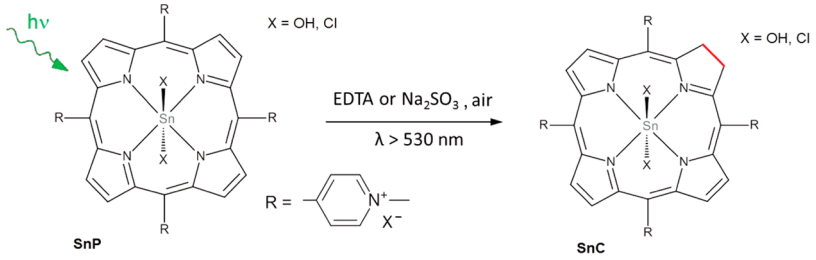

Scheme 2. Photocatalytic System for the Reduction of $BNAD^+$ Applying Tin(IV)-*meso*-tetrakis(*N*-methylpyridinium)-chlorin (SnC) as a Red-Light Responsive Multielectron Transfer Sensitizer Able To Recycle the Selective Hydride Transfer Mediator $[Cp^*Rh(bpy)H]^+$ in Neutral Aqueous Solution

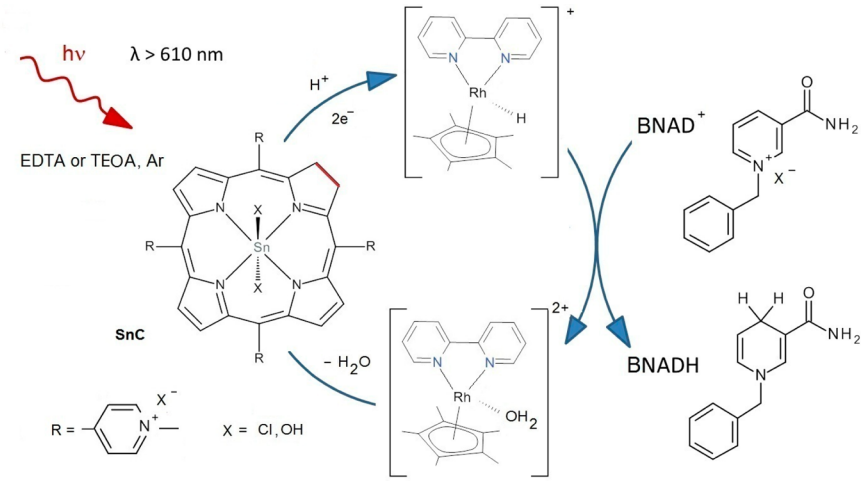

conversion, while, at the same time, solving the putative difficulties of a gradual chlorin accumulation. The axial coordination sphere of the central metal of such photosensitizers may be easily varied independently for further modifications of the systems such as immobilization or coupling to other functional subunits including co-catalysts, depending on the nature of the substituents X.[13,14,20−24] Moreover, in a wavelength-controllable process, the readily accessible tin porphyrin precursor complexes SnP, which can be considered as the long-term stable resting states of this class of multielectron transfer photosensitizers under ambient conditions, can be conveniently transformed in situ to the corresponding hydrogenated chlorin species SnC (Scheme 1).[25] Here, we show that the metallochlorin complexes obtained may then be selectively excited with red light for photocatalytic (B)NADH formation (Scheme 2).

2. RESULTS AND DISCUSSION

2.1. Synthesis and Characterization of the Tin Porphyrin Precursor Complex. The starting material tin(IV)-*meso*-tetrakis(*N*-methylpyridinium)-porphyrin (SnP with X = Cl, Scheme 1) was prepared and characterized according to the reported literature procedure.[26] Depending on the specific synthesis and purification conditions of such compounds, different metalloporphyrin derivatives containing an undesired mixture of axially bound ligands X such as chloro and hydroxy groups may sometimes be formed and isolated.[27,28] Moreover, under reductive conditions, the axial chloro ligands bound to the high-valent central metal of tin(IV) porphyrins have been shown to become labile against hydrolysis.[29] For our investigations with water-soluble tin porphyrin derivatives, the actual nature of the axially bound ligands X was therefore additionally studied via solid-state ^{119}Sn NMR of the isolated compounds (Figure 1), where only one resonance occurred, at −588.3 ppm. A comparison of the chemical shift of this signal with the literature data for the closely related tetraphenylporphyrin complex $Sn(TPP)Cl_2$ in $CDCl_3$ (δ = −589 ppm) leads to the conclusion that, in our SnP samples, two chloride ligands are attached to the tin(IV) central atom.[30,31] More importantly, the corresponding ^{119}Sn NMR chemical shift was also observed in neutral aqueous solution of the SnP compound at 298 K. This finding clearly indicates that, at neutral pH, the complex is not immediately hydrolyzed to form a dihydroxo tin species with X = OH. In order to further study the conditions required for such an axial ligand exchange, subsequently, 10 μL of KOH (c = 2 mol/L) were added, and a broadened and downfield-shifted (deshielded) ^{119}Sn resonance occurred at −585.5 ppm. At this stage of the reaction, the increased line width of the ^{119}Sn resonance peak might reflect a higher asymmetry around the ^{119}Sn metal center and, therefore, indicate the occurrence of a stepwise exchange process of the axial chloro ligands against hydroxyl groups, as observed previously by mass spectroscopy with related main group metalloporphyrin complexes.[32] After the addition of further 10 μL of the concentrated KOH solution, finally a chemical shift at −579.1 ppm was reached.

dx.doi.org/10.1021/ic401611v | Inorg. Chem. 2013, 52, 11910−11922

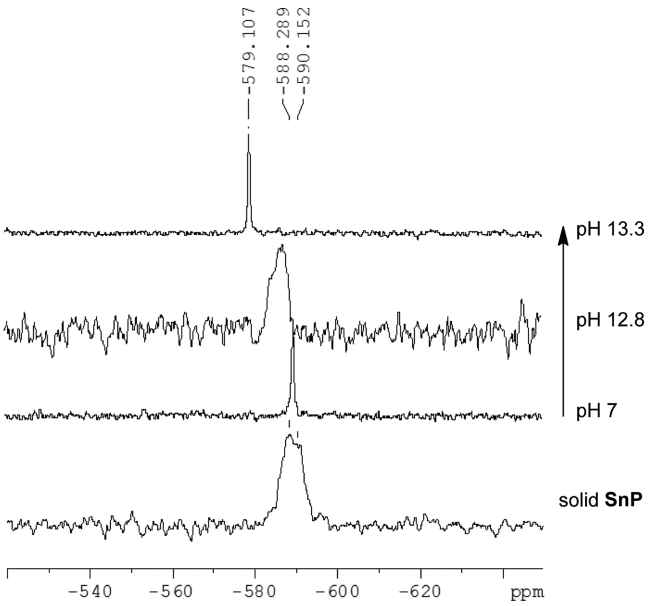

Figure 1. ^{119}Sn NMR spectra of tin(IV)-*meso*-tetrakis(*N*-methylpyridinium)-porphyrin (SnP) in the solid state and in H_2O:D_2O = 9:1 with increasing pH values.

The sharp peak at −579.1 ppm indicates the complete exchange of two axial chloro ligands by hydroxide ions.[30,31]

Additional ^{1}H NMR experiments in neutral aqueous solution also showed no evidence for axially attached hydroxide ligands, since there were no proton resonances found between 0 and −10 ppm.[28] Only under more-alkaline conditions (pH 12, Figure 2) could a gradual evolution of a single proton signal at

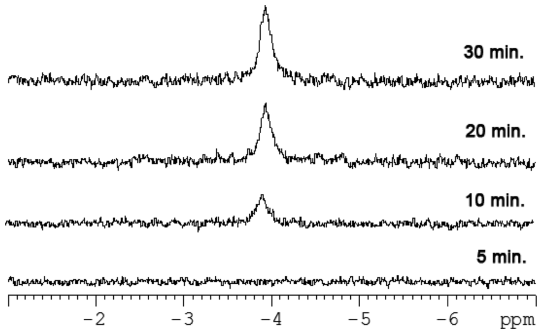

Figure 2. ^{1}H NMR spectra of tin(IV)-*meso*-tetrakis(*N*-methylpyridinium)-porphyrin (SnP) dissolved in H_2O/D_2O = 9:1 at pH 12.1. The increase of the single proton signal at −3.85 ppm indicates the gradual exchange process of axial chloride by hydroxide with time.

−3.85 ppm be observed, indicating the occurrence of an exchange process from chloride to hydroxide ligation. Despite of the enormous stability typical for high-valent tin porphyrins,[14,33] further addition of KOH finally led to a demetalation of the SnP compound. As a consequence, the ^{119}Sn signal at −579.1 ppm fully vanished, while at the bottom of the NMR tube, a solid gray precipitate was formed, which was not further characterized.

The pH-dependent exchange processes of axial ligands X in SnP in aqueous solution were also studied by ultraviolet−visible light (UV-vis) spectroscopy (see the Supporting Information). In the pH range of 6−10, the 422-nm Soret-band absorption maximum of the tin(IV)-*meso*-tetrakis(*N*-methylpyridinium)-porphyrin complex with X = Cl remained essentially constant. At pH >10, the spectroscopic titration experiments resulted in a small bathochromic shift of the Soret-band to 424 nm, which, consistent with our proton NMR data, is interpreted as the formation of the dihydroxo species with X = OH. In acidic solution (at pH 4−6), we could verify a reversible protonation step of the dichloro-substituted tin(IV) complex of the *meso*-tetrakis(*N*-methylpyridinium)-porphyrin cation as indicated by a hypsochromic shift of the Soret band, which has been previously described and tentatively interpreted in the literature as a process occurring at one of the central porphyrin nitrogen atoms.[34]

Taking together all these results, we have evidence that the photocatalyst precursor SnP studied in our system is initially carrying axial chloro ligands (X = Cl), since the pH value in all experiments carried out in buffered aqueous systems was kept between pH 7 and pH 9 in order to maintain the stability of the investigated nucleotide co-factors. Under the photocatalytic reaction conditions reported here, however, the intermediate formation of aromatic ring-reduced species will certainly allow an exchange of axially bound chloride with other ligands such as hydroxide.[29] Interestingly, even a direct inner-sphere interaction with the rhodium co-catalyst in the axial coordination sphere of the tin complex cannot be excluded, as will be discussed later.

2.2. Formation of the Tin Chlorin Photosensitizer.

Upon visible-light irradiation in the presence of suitable electron donors (Scheme 1), the water-soluble tin(IV)-complex of *meso*-tetrakis(*N*-methylpyridinium)-porphyrin (SnP) can be selectively reduced under ambient conditions to generate the tin(IV)-*meso*-tetrakis(*N*-methylpyridinium)-(2,3-dihydroporphyrin) or the chlorin derivative SnC (Scheme 1). This clean and rapid transformation, which can be driven to completeness, is easily followed by UV−vis spectroscopy and characterized by the occurrence of several isosbestic points (see the Supporting Information). Upon irradiation with green light in the presence of dioxygen, a photochemical quantum yield of $\varphi = 4 \times 10^{-3}$ was obtained for the chlorin formation process, using 0.01 M EDTA as an electron donor (298 K; light-emitting diode (LED) wavelength of 525 nm). A more efficient route to obtain the chlorin species is the photochemical reduction with sodium sulfite added as an electron donor in basic aqueous solution, which is also carried out under ambient conditions. Following this approach, a very promising quantum yield of up to φ = 0.34 could be achieved for the in situ generation of the photosensitizer SnC. Sulfate was identified as the oxidation product of the sacrificial two-electron donor sulfite (for more details, see the Supporting Information).

As expected for this class of compounds,[35−37] reducing one of the pyrrole rings of the SnP precursor complex to form the metallochlorin (2,3-dihydroporphyrin) derivative SnC results in characteristic effects on the absorption band pattern in the visible spectrum (see Figure 3).

The tin chlorin compound displays a strong absorption peak in the red spectral region (Q_y-band), and several less pronounced absorptions at wavelengths of <600 nm, which resembles the spectrum of native chlorophyll derivatives such as Chl *b* (also shown in Figure 3). With regard to the SnP precursor, this enhanced red-light-harvesting feature of the corresponding tin chlorin complex SnC is also reflected by the deep green color of the photosensitizer in solution. Such a sufficiently red-shifted threshold wavelength (here, with an absorption onset at λ_{thr} = 660 nm or E = 1.88 eV) can be

dx.doi.org/10.1021/ic401611v | *Inorg. Chem.* 2013, 52, 11910−11922

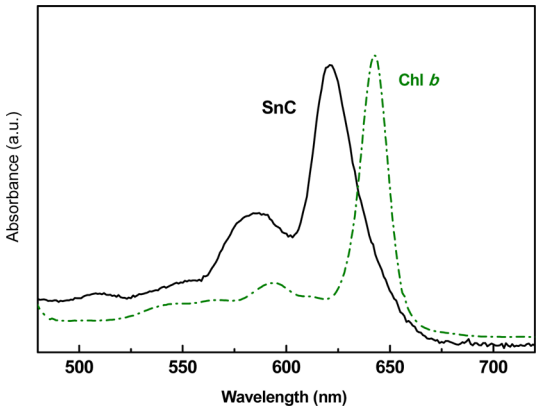

Figure 3. Comparison of the Q-band absorption pattern of the water-soluble tin(IV)-*meso*-tetrakis(*N*-methylpyridinium)-chlorin complex SnC (solid line) with the visible-light-harvesting features of native chlorophyll *b* from natural photosynthetic antenna proteins, showing a comparable threshold wavelength at ~660 nm (denoted by the dashed line).

regarded as one of the key requirements for potential solar energy conversion applications such as artificial photosynthesis.[2,38] It should also be mentioned, in this context, that, in contrast to the natural chlorophylls, which display quite similar spectral features but an adaptation to biological energy conversion conditions, the biomimetic photosensitizers reported here are characterized by an excellent water-solubility and turned out to be extremely robust against demetalation and degradation processes.

2.3. Photocatalytic Reduction of Nucleotide Co-factor Analogues. The artificial photosynthetic production of *N*-benzyl-1,4-dihydro nicotine amide (BNADH) was powered by green- or red-light irradiation and carried out under an argon atmosphere (see Scheme 2). For this purpose, buffered aqueous solutions of the oxidized nucleotide co-factor model $BNAD^+$ (1 mM) containing a catalytic amount of the SnC photosensitizer (typically in the micromolar range) were mixed with an excess of sacrificial electron donors such as TEOA or EDTA. The concentrations of all components were kept low enough to be able to follow the photocatalytic process spectroscopically under continuous-wave irradiation without any further dilution steps. As an additional redox mediator, the rhodium complex [Cp*Rh(bpy)Cl]Cl was added. In aqueous solution,[39] the complex $[Cp^*Rh(bpy)H_2O]^{2+}$ is formed (Scheme 2), which has already been extensively studied as an electrocatalyst for regioselective NAD^+ hydrogenation.[10] This selective catalytic process involves the participation of a hydrido-rhodium intermediate $[Cp^*Rh(bpy)H]^+$ exclusively generating the enzymatically active 1,4-NADH form of the reduced co-factor.[10,39,40] Recently, it has been shown that such rhodium complexes can also be incorporated in light-driven redox systems based on different types of sensitizers.[9,41−43] Here, we are employing this type of redox mediator to enable a photocatalytic reduction of the nucleotide co-factor model compound $BNAD^+$,[44] which was added to the system as chloride salt in buffered aqueous solution.

In the presence of SnC as a sensitizer, a photocatalytic accumulation of the two-electron reduced compound BNADH was indicated by a new absorption band between 320 and 360 nm (ε = 7240), which continuously increased under steady-state irradiation with visible light (Figure 4). No such reaction was observed in darkness or without SnC or the rhodium mediator present. After the photolysis experiments, luminescence measurements showed a broad new emission band at 470 nm upon excitation of the sample at 340 nm, which could also be verified by the corresponding excitation spectrum (Figure 4). These findings can also be ascribed to a successful photochemical synthesis of BNADH.[45]

In the experiment shown, the total increase of the product absorption band corresponds to ~15% conversion of the oxidized $BNAD^+$ co-factor initially added (1 mM). Therefore, it

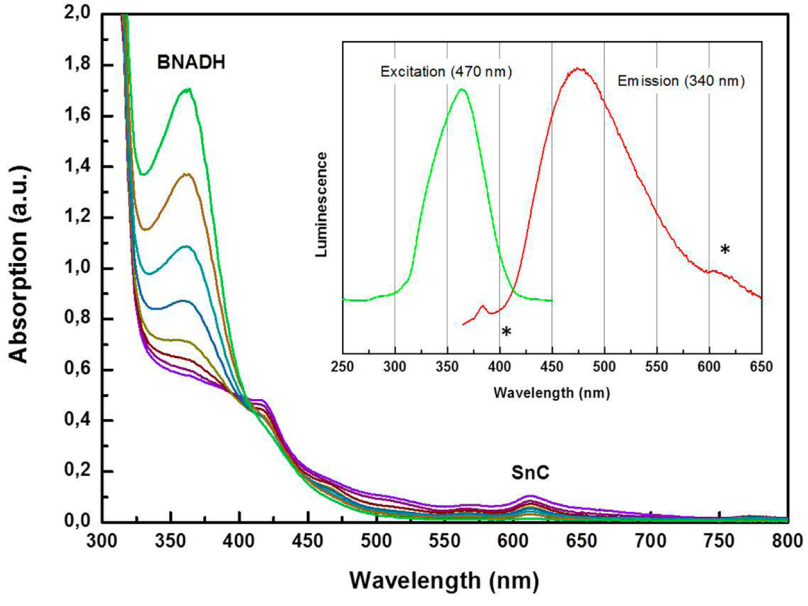

Figure 4. Spectral changes observed during visible-light irradiation (λ > 530 nm, 298 K, 1 cm cell) of an anaerobic aqueous solution containing 1 mM $BNAD^+$, $[Cp^*Rh(bpy)H_2O]^{2+}$, EDTA, and a small amount of the tin chlorin complex SnC as the photosensitizer (6×10^{-6} M). Inset: Luminescence and excitation spectra of the BNADH photoproduct accumulated in the course of the photocatalytic process (the asterisk marks artifacts due to minor SnC reabsorption and fluorescence).

dx.doi.org/10.1021/ic401611v | *Inorg. Chem.* 2013, 52, 11910−11922

is clear that the reaction is catalytic, both in terms of the tin chlorin photosensitizer (6 μM, log ε = 4.25 at the Q_y-band maximum),[25] as well as the rhodium co-catalyst present in solution. From the spectroscopic data of the photolysis shown in Figure 4, a lower limit for the average turnover number (TON) of BNADH molecules produced per each photosensitizer molecule (the minimum number of turnovers completed up to this point)[46] can be estimated as TON(SnC) = 28. We also measured the quantum yield of this process using selective red-light (Q_y-band) excitation (see the Supporting Information). A value of $\varphi = 3 \times 10^{-4}$ was obtained for the BNADH formation reaction monitored by the increase of UV absorption (298 K, LED: 623 nm). This value (calculated here as a lower limit by assuming only one mole of incident photons required per mole of product molecule formed)[47] is in the order of magnitude of other photocatalytic co-factor recycling systems reported recently, which were powered by blue-light radiation.[43,48]

Frequently, the formation of the reduced nicotinic acid moiety of nucleotide co-factors and related model compounds such as BNADH is only characterized by the type of diagnostic electronic spectral features reported above. Typically, an appearance of the optical absorbance band at 340 nm and sometimes also the corresponding luminescence signal at ~470 nm are utilized for the quantification of NADH derivatives in bioanalytical assays. Under abiotic conditions, however, following these spectroscopic signatures alone could be misleading, since other reaction products such as biocatalytically inactive isomeric forms or undesired co-factor dimerization products with similar spectroscopic features might also be obtained. Therefore, the usefulness of potential NADH regeneration systems is sometimes verified with an appropriate enzymatic assay, where the reduced co-factor is consumed and thus indirectly monitored via substrate conversion. We also did so within the case of artificial photosynthetic NADH production, and the results are presented in the next sections. For an unambiguous direct quantification of the accumulated model compound BNADH, a combination of different analytical methods was chosen here. It has been shown previously that the regioselective reduction of synthetic nucleotide co-factor substitutes such as $BNAD^+$ to the corresponding 1,4-dihydro form can be analyzed using high-performance liquid chromatography (HPLC), nuclear magnetic resonance (NMR), and electrospray ionization–mass spectroscopy (ESI-MS).[48,49] Therefore, we also decided to apply an additional high-performance liquid chromatography/high-resolution mass spectroscopy (HPLC/HRMS)-based detection method for the confirmation and characterization of the obtained photoreduction products. The details of these further control experiments are described in the Supporting Information.

2.4. Photocatalytic Reduction of Natural NAD^+ Co-factors. The application of the artificial photosynthetic co-factor recycling system described above was extended to study also the visible-light-driven reduction of natural NAD^+ under slightly different conditions, which were systematically varied to get more insight into the mechanistic details of the process. Long-wavelength irradiation was performed with a 150 W xenon lamp equipped with suitable cutoff filters or with a high-power LED setup (see the Supporting Information) and approached in three different ways. First, experiments were starting directly from the tin porphyrin precursor complex SnP in nitrogen-saturated solution, which allowed us to gain more insight into the oxygen-sensitive steps of the tin chlorin formation sequence summarized in Scheme 1. In another set of experiments, the photolysis was performed with the tin chlorin photosensitizer SnC produced via photochemical reduction with EDTA under ambient conditions prior to the addition of other reagents to the sample and purging with argon. The third variation of photocatalytic reaction conditions was based on the use of anaerobic aqueous SnC solutions obtained from sulfite reduced SnP already described in the previous sections.

An experiment starting directly from photoexcited SnP in the presence of EDTA as the electron donor is shown in Figure 5.

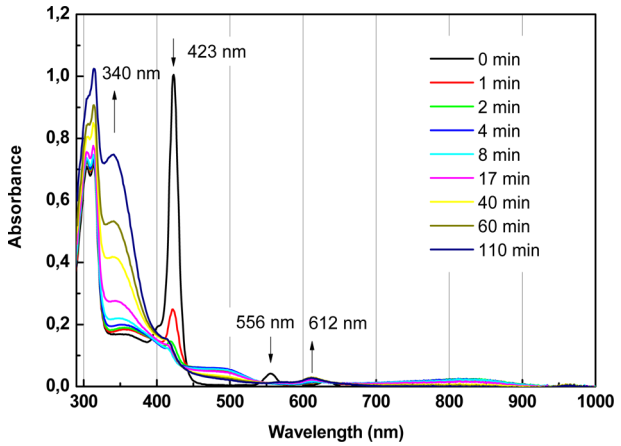

Figure 5. UV–vis and NIR spectral changes of a solution containing SnP, NAD^+, EDTA, and $[Cp^*Rh(bpy)H_2O]^{2+}$ under N_2 in 0.1 M phosphate buffer pH 7.4, using a 150 W xenon lamp light source with a 530-nm cutoff filter. The initially increasing absorbance at 840 nm indicates that tin-phlorin species[50] are formed first under these conditions. After a few minutes, the chlorin complex SnC and also higher reduced tetrahydroporphyrin species accumulate. Irradiation of these compounds then starts to accelerate the reduction of NAD^+ to NADH visible at 340 nm. The results shown correspond to a turnover number of TON > 72 for co-factor photoreduction based on the initial amount of SnP.

Note that the rhodium complex added as an additional redox mediator shows a characteristic absorption pattern in the 300–320 nm range. At the beginning of the reaction, a rapid depletion of the metalloporphyrin Soret bands and Q-bands at 423 and 556 nm, and the rising of a broad new NIR-band with a maximum at 840 nm is observed. In agreement with the typical behavior reported for other tin porphyrins in the literature,[19] these spectral variations indicate that, in the first reaction sequence, the air-sensitive *meso*-hydrated tin(IV)-phlorin (5,24-dihydroporphyrin) derivative[19,50] is formed as a primary reduction product of SnP in deaerated solution, which then rearranges to form the oxygen-stable metallochlorin species SnC. In aerobic solution, only the overall SnC formation process can be monitored under steady-state irradiation conditions, according to Scheme 1 (see the Supporting Information).

It turned out that several additional cross-reactions are possible, which could be explored separately by a selective excitation of the steady-state chromophore mixture present in solution using different cut-off filters or LED-light sources, providing nearly monochromatic wavelengths. When, for example, a 530-nm cutoff filter is used as shown in Figure 5, the Q-bands of SnP are also excited, and a product-consuming back reaction of NADH competing with the sacrificial electron

dx.doi.org/10.1021/ic401611v | *Inorg. Chem.* 2013, 52, 11910–11922

donor EDTA can take place, thus forming NAD^+ and reduced tin porphyrin species. Such a photoreduction of tin porphyrins with NADH as a donor, which has been reported previously in earlier work,[16] can explain the apparent lag-phase of NADH production in the systems starting with SnP instead of SnC as the photosensitizer. Furthermore, depending on the type and excess of sacrificial electron donor applied under photocatalytic conditions, also a certain amount of a higher reduced metalloporphyrin species carrying partially or fully protonated tetrahydroporphyrin ligands may accumulate as an additional side product besides the desired tin chlorin complex SnC. In Figure 5, such a process is reflected by the rising Q_y-band pattern in the 600–650 nm region. While the SnC derivative shows a maximum at ~633 nm, the additional peak rising at 612 nm can be tentatively attributed to the presence of a tin(IV)-complex carrying an adjacent tetrahydroporphyrin or *meso*-tetrakis(*N*-methylpyridinium)-isobacteriochlorin type of ligand.[35,36] As will be shown below, however, at slightly higher pH, this reversible pyrrole ring protonation process[36] involving the 7,8-position of the chlorin ligand can be suppressed to a significant extent. Despite all of these inevitable complications consuming some of the reduction equivalents, a new absorption band at 340 nm is clearly rising under photostationary conditions (Figure 5), which indicates the reduction of NAD^+ to NADH. A lower limit of TON > 72 for the turnover number achieved was calculated from the tin-porphyrin-derived maximum amount of SnC photosensitizer that can be present in the reaction mixture. This value was estimated from the optical spectra, assuming the molar absorption coefficient of NADH at 340 nm to be ε = 6300 mol^{-1} cm^{-1} (taken from literature data).[45]

Later experiments with SnC as the photocatalyst obtained directly from the sulfite-reduced SnP species with either EDTA or TEOA as a donor resulted in comparable or higher NADH yields. As an example, in Figure 6, the photolysis of such a tin-chlorin-containing aqueous solution with a very small excess of EDTA as the electron donor is shown.[51] There are still

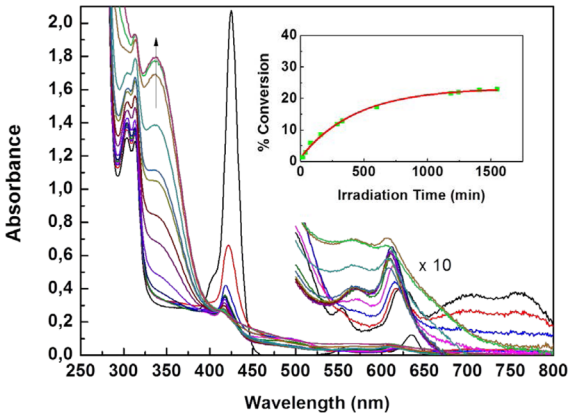

Figure 6. UV-vis spectral changes of a solution containing 7.5 μM SnC obtained by sulfite reduction of SnP; 1 mM NAD^+; 0.01 M EDTA and 7.7×10^{-5} M $[Cp^*Rh(bpy)OH]^+$ under argon in 0.1 M phosphate buffer pH 8.8; 150 W Xe lamp with 590 nm cutoff filter; 298 K. Note that, in contrast to Scheme 2, water ligands bound to the rhodium site (pK_a = 8.2)[39] are deprotonated at pH 8.8. After 25 h of irradiation, almost no more changes of the spectra are observed (the trace with the highest amount of NADH was recorded at 48 h). Numbers shown for % conversion are given relative to the total initial amount of NAD^+. TON(SnC) = 30.

significant amounts of the initial porphyrin precursor SnP visible (in the present case, up to 40%, upon estimation by the residual absorbance at 556 nm). The remaining metalloporphyrin absorption bands usually disappear within 1 min of steady-state photolysis in all observed cases, because of the photochemical formation of different reduced porphyrin species, as already discussed above.

During photolysis of a solution containing only 0.01 M EDTA as a sacrificial donor, the reaction sensitized by SnC typically reaches a plateau slightly above 20% of conversion of the initial amount of NAD^+ (see inset of Figure 6). Interestingly, almost identical equilibrium conditions were found, when the excitation wavelength was further red-shifted (610 nm cutoff filter) to avoid an irradiation of any remaining SnP. It could be assumed that, under the conditions of very low excess of EDTA, as shown in Figure 6, the photocatalytic process is presumably limited by the amount of the primary reductant. Therefore, we decided also to vary the type and concentrations of sacrificial electron donors. Indeed, when larger amounts of EDTA were present, the product accumulation proceeded faster and much higher conversion yields of more than 70% NADH were readily achieved within a single run (see Figure 7). A similar performance was also

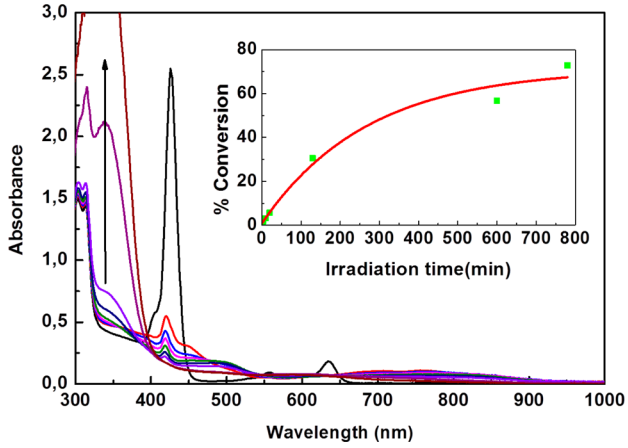

Figure 7. UV-vis and NIR spectral changes of a solution containing 7.5 μM SnC obtained by sulfite reduction of SnP; 1 mM NAD^+; 1 M EDTA, and 7.7×10^{-5} M $[Cp^*Rh(bpy)OH]^+$ under argon in 0.1 M phosphate buffer pH 8.8; 150 W Xe lamp with 610 nm cutoff filter; 298 K; 73% conversion to NADH and TON(SnC) = 97 are reached.

observed with TEOA as the electron donor under otherwise identical conditions (Supporting Information). These findings suggest that a more-pronounced reductive quenching of the excited-state SnC sensitizer, thought to be responsible for initiating the subsequent co-factor reduction process, is reached with a larger excess of electron donor.

As an additional control experiment to further support the successful accumulation of NADH, in some cases, the time-dependent changes in luminescence spectra were also followed in the course of the photocatalytic process (Figure 8). These data are consistent with the co-factor conversion profiles obtained from UV-vis spectroscopy.

From the linear region of the irradiation time profiles typically observed within the first hours of exposure to red light (Figure 9), an initial turnover frequency of TOF > 20 h^{-1} can be estimated, which corresponds to a calculated space-time-yield of 2.5 g L^{-1} d^{-1} of NADH in these cuvette-based

dx.doi.org/10.1021/ic401611v | *Inorg. Chem.* 2013, 52, 11910–11922

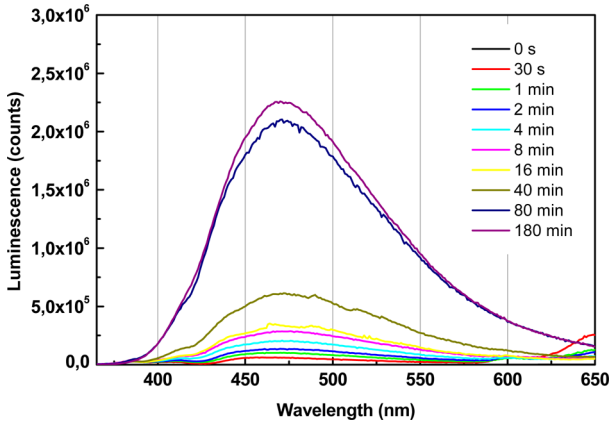

Figure 8. Luminescence spectra of a solution containing 7.5 μM SnC; 1 mM NAD^+; 15 w/v% TEOA and 7.7×10^{-5} M $[Cp^*Rh(bpy)OH]^+$ under argon in 0.1 M phosphate buffer pH 8.8; 150 W Xe lamp with 610 nm cutoff filter; increasing luminescence upon excitation at 340 nm exhibiting a maximum at λ_{max} = 470 nm indicates the reduction of NAD^+ to NADH.

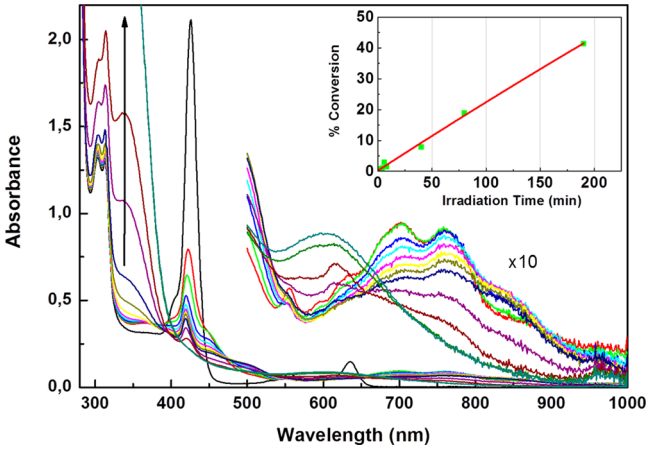

Figure 9. UV−vis and NIR spectral changes of a solution containing 7.5 μM SnC; 1 mM NAD^+; 15 w/v% TEOA (1 M) and 7.7×10^{-5} M $[Cp^*Rh(bpy)OH]^+$ under argon in 0.1 M phosphate buffer pH 8.8; 150 W Xe lamp with 610 nm cutoff filter; TON(SnC) = 56 after 5 h (see the Supporting Information).

laboratory-scale experiments.[52] Nevertheless, very promising absolute product formation quantum yield values between 1% and 2% were obtained for the artificial photosynthetic formation of NADH. As an example, in Figure 9, the initial reaction period of photocatalytic product accumulation with SnC as a sensitizer, $[Cp^*Rh(bpy)H_2O]^{2+}$ in its deprotonated form as a redox mediator and TEOA as a sacrificial electron donor is shown together with the spectral variations observed. These data correspond to a NADH-production quantum yield of φ = 0.014 (298 K, LED: 592 nm). In this context, it is worthwhile to compare this value with the absolute quantum efficiencies determined for the photoaccumulation of reduced chemical species in natural photosynthetic systems, which are typically reaching maximum values of φ = 0.01−0.06 in a comparable spectral region.[53−55]

At the current stage, we have not yet tried to optimize the NAD^+ to $[Cp^*Rh(bpy)H_2O]^{2+}$ ratio of the photocatalytic reaction mixtures. It has been shown, however, in a recent publication describing a related blue-light powered NADH recycling system,[43] that up to 100% conversion yields of NAD^+ are possible when the relative concentration of the rhodium mediator is increased. Therefore, we believe that our current limit of ~0.5 g L^{-1} NADH obtained from 1 mM NAD^+ starting solutions (Figure 7) could still be further improved in a similar way.

One of the most significant findings in our case, however, besides the fact that the catalysis can be powered by red light, is the excellent long-term stability of the multielectron transfer sensitizer used. As displayed in Figure 10, the starting spectrum

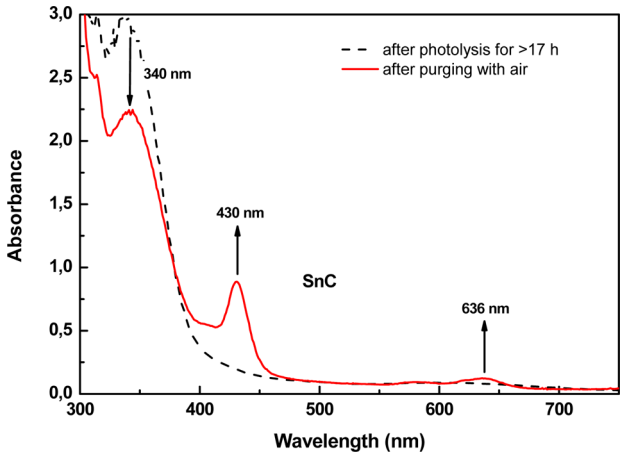

Figure 10. Typical UV-vis spectra of a photostationary mixture recorded after successful NADH accumulation in a long-term photolysis experiment performed with 15 w/v% TEOA as the electron donor. As can be seen, the chlorin photosensitizer SnC is immediately recovered by oxidation with air (solid line). The small peaks between 300 and 320 nm indicate that also the rhodium-based redox mediator is still intact. Note that only the product absorption band at 340 nm decreases significantly, because of the oxygen sensitivity of NADH.

of the green SnC complex is easily restored after driving the NADH production process to the maximum yield of a single long-term irradiation experiment. Purging the anaerobic photostationary mixture of reduced metalloporphyrin derivatives with air obviously leads to a reoxidation of all intermediate photosensitizer reduction products back to the tin chlorin derivative, as indicated by the reappearing Soret-band and Q-band maxima at 430 and 636 nm (see Figure 10). Upon subsequent addition of HCl, the overlapping 340-nm band of the acid labile photoproduct NADH[56] could be completely removed to better analyze also the UV region of the spectrum, where the rhodium mediator absorbs characteristically (not shown here). These types of experiments support the belief that the apparently photobleached SnC is still fully intact, even after extended irradiation times with 40 h of exposure to light or longer. Such a promising stability behavior of the key components of this artificial photosynthetic system will certainly open the stage for a repetitive series of long-term NAD^+ photoreduction cycles in order to increase the total yield of the reduced co-factor. Corresponding experiments to characterize the absolute TON limits[46] of the catalysts applied therefore still must be performed. However, such long-term irradiation experiments were not yet within the scope of our work, which was more focused on the mechanistic aspects of this novel photocatalytic reaction sequence.

2.5. Coupling Artificial Photosynthesis of NADH to an Enzymatic Process. The light energy stored in the form of NADH equivalents can be utilized for powering other

endergonic substrate conversion processes in subsequent "dark reactions". If any enzymatically accelerated steps must be involved for this purpose,[3,5] it is important to demonstrate that the energy-rich nicotine amide compound provided, and the reaction conditions selected, are indeed compatible with the limiting constraints of such biochemical processes. As an additional confirmation of the regioselective co-factor recycling process, the photocatalytic 1,4-NADH synthesis reaction reported in this work was, therefore, also coupled to a simple enzymatic assay. For this purpose, we selected the NADH-dependent yeast enzyme alcohol dehydrogenase (ADH, EC 1.1.1.1.) from *Saccharomyces cerevisiae*,[57] which can be applied to reversibly convert different carbonyl compounds such as acetone, acetaldehyde, and butyraldehyde to the corresponding alcohols.[58] While interesting light-independent co-factor recycling processes to provide chiral ketone reduction products have also been reported in the literature,[59] it should be pointed out that we have chosen here a more simple reaction sequence to serve merely as a clear proof of principle for our concept. Nevertheless, several important aspects must be considered in such a hybrid biophotocatalytic reaction system. The performance of any enzymes to be coupled is usually characterized by a limited temperature and pH range and a substrate-dependent variation in efficiency. Furthermore, the enzymatic process may be severely disturbed by various substances present only under abiotic reaction conditions. For example, the zinc-enzyme ADH is well-known to be inhibited by Zn^{2+} chelating compounds such as 2,2′-bipyridine (bpy) and EDTA, which are at least partially present as functional components in all of the photocatalytic systems applied here (Scheme 2). Moreover, the natural function of several enzymes may turn out to be significantly modified or even completely inactivated when the biocatalysts are exposed to light under artificial reaction conditions.[2] Despite of these possible limitations, we could successfully couple the photocatalytic NADH generation process to a subsequent enzymatic alcohol production step catalyzed by ADH. Different ways to provide the active photosensitizer SnC, as discussed in the sections above, were tested in the enzymatic assays. The obtained alcohols were quantified by gas chromatography with acetonitrile added as an internal standard. For analytical reasons, we started to monitor the formation of isopropanol qualitatively from acetone as a substrate using photochemically reduced NAD^+ as a redox co-factor and alcohol dehydrogenase as the biocatalyst accelerating the coupled dark reaction. However, it is well-known that the activity of ADH for the conversion of acetone is comparably low.[60] Even though it could be demonstrated that the expected biophotocatalytic reaction sequence is working properly, the best results achieved in the isopropanol production system therefore resulted only in unsatisfactory turnover numbers. In contrast, the application of our photochemical system to the production of *n*-butanol from butyraldehyde (*n*-butanal) was much more successful, and turnover numbers referred to the limiting amount of tin chlorin photocatalyst of TON(SnC) > 100 could be readily achieved. A typical example for such an enzyme-coupled photocatalytic experiment is shown in Figure 11. For this plot, the sample was irradiated in a 1-cm cuvette sealed with a septum to directly compare these results with the reaction conditions of the other experiments shown in the previous sections. Within the first 90 min of irradiation, an *n*-butanol concentration of ∼1 mM is built up, which corresponds to a turnover number of TON > 130 of completed photoreaction cycles up to this time. This lower limit value is

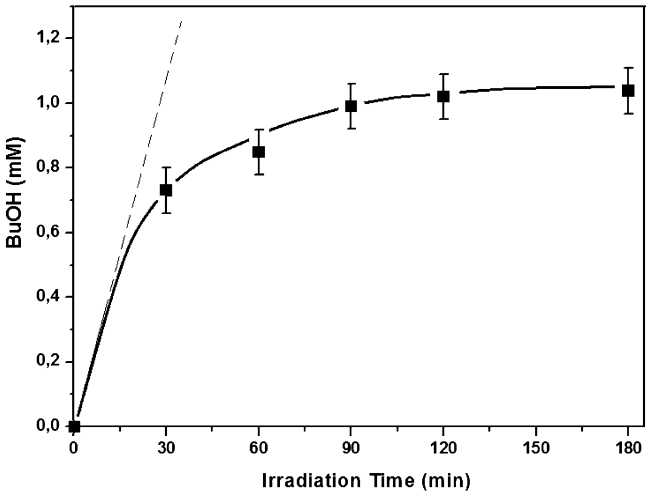

Figure 11. Time profile for the formation of *n*-BuOH in the NADH-dependent photoenzymatic reduction of butyraldehyde using SnC as the photosensitizer (see text).

based on the initial concentration of the multielectron transfer sensitzer SnC and assuming a 1:1 ratio of NADH required for each two-electron reduced aldehyde molecule.[47]

If NADH-based reduction equivalents are generated in the system, the reversible enzymatic process catalyzed by ADH should be able to reach the pH-dependent equilibrium between the aldehyde and alcohol substrate.[57] We assumed that, under the chosen reaction conditions (see the Experimental Section), the observed product formation rate should be limited by the quantum yield of NADH generation in the absence of the enzyme.

The reaction progress was followed by UV-vis spectroscopy and gas chromatography (GC) measurements. In contrast to the experiments described in the previous sections, the 340-nm signal of NADH was no longer built up significantly upon photolysis in the presence of ADH. The total amount of enzyme in the system was set comparably high (∼210 U) in order to guarantee sufficient catalytic activity also in the solution containing an excess of free EDTA, which may affect the active site of the ADH by competitive zinc-ion complexation, as already mentioned previously.[60] As can be seen (Figure 11), the alcohol product formation rate rapidly decreases within the first hour of irradiation, approaching an equilibrium concentration. The initial rate of *n*-BuOH production is ∼2 mM h^{-1} (33 U of net "photo-enzymatic" activity), corresponding to a turnover frequency of TOF = 266 h^{-1}, based on the SnC photosensitizer, which compared to the maximum values of light-independent systems reported in the literature is quite promising (TOF < 30 d^{-1}).[59] Interestingly, this TOF value is also more than 10 times higher than the typical range of values observed in the NADH accumulation experiments described in the previous sections, where the loss of stored chemical energy by back-reactions seems to be more dominant. Although the absolute quantum yield determination for monochromatic irradiation has not yet been carried out, it can already be concluded from the data shown above (see Figures 6 and 7) that the permanent product formation in the presence of ADH is occurring with a mean quantum yield of $\varphi \approx 0.1 \pm 0.05$, estimated for red-light irradiation, which is within a reasonable order of magnitude, compared to the action spectra of photosynthetic systems.[55] We ascribe this enormous improvement in efficiency to the effect of immediately utilizing

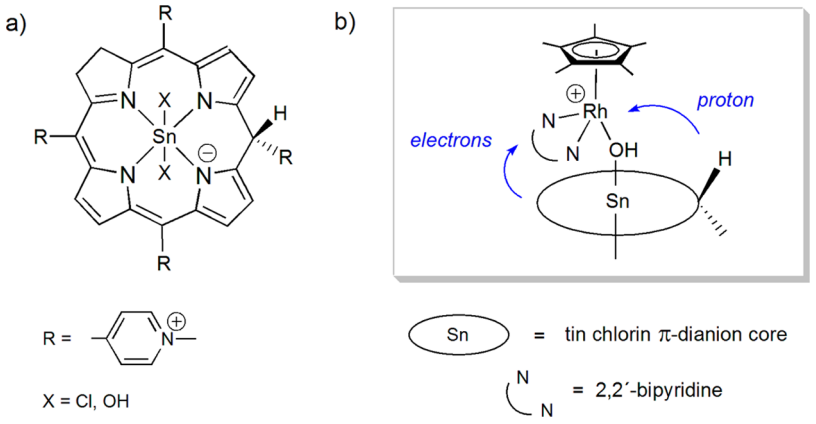

Figure 12. (a) Molecular structure of the proposed tin(IV) chlorin-phlorin anion complex $SnCH^-$, which, according to the literature,[65] represents the most plausible tautomeric form of a two-electron ring-reduced *meso*-protonated derivative of the chlorin photosensitizer SnC. (b) Possible axial interactions of $SnCH^-$ with the co-catalyst leading to SnC regeneration and rhodium-hydride complex formation, similar to the reduction pathways proposed for electrocatalysis[39] or the reaction of the $[Cp^*Rh(bpy)H_2O]^{2+}$ catalyst precursor with HCO_2^- as the hydride source.[40]

the photogenerated NADH with an additionally coupled two-electron redox process in situ as soon as it is formed. This coupling competes with possible side reactions and helps to avoid a loss of the chemical energy stored caused by the limited long-term stability of the reduced co-factor. It is well-known that quite similar strategies to preserve the intermediately stored reduction equivalents carried by the NADH co-factor are operating in the carbon dioxide reduction cascade (Calvin cycle) and also in the cyclic electron flow processes occurring in natural photosynthesis.[61,62] It is important to mention here also some of the control experiments carried out, which showed that a photolysis under the same conditions as described above (Figure 11), but without the enzyme and NAD^+ present, did not lead to any observable *n*-BuOH formation. Nor did a dark sample containing all functional components result in any variations of the UV–vis absorption spectra or indicate any formation of the alcohol product.

While the light-driven reaction cascade discussed here is certainly not yet performed under optimized conditions, the present results clearly demonstrate that an efficient regioselective photocatalytic reduction of the nucleotide co-factor NAD^+ required for the coupling to an enzymatic process has been achieved. Other types of "dark reactions", which are more relevant in the context of artificial photosynthesis and solar energy conversion such as NADH-dependent abiotic CO_2-fixation processes[2,5] will now also be tested with this type of biomimetic photocatalysis.

2.6. Aspects of Multielectron Transfer Sensitization and Hydride Transfer: A Tentative Reaction Mechanism.

In the study presented here, a systematic variation of the reaction parameters, including pH, electron donor supply, and excitation wavelengths, has been performed in order to elucidate the conditions required for an efficient photocatalytic recycling of nucleotide co-factors. It turned out that a complicated sequence of additional reactions coupling the light-induced primary processes of the photoexcited tin chlorin SnC with further electron transfer and protonation steps is necessary to enable the accumulation of NADH. Nevertheless, an attempt is made here to provide a simplified mechanistic picture, which, to the best of our knowledge, is fully consistent with the available literature and all of our experimental and spectroscopic data.

Upon irradiation with visible light absorbed only by the sensitizer, the photocatalytic process is initiated by reductive quenching of photoexcited SnC with an electron donor D. This photoinduced electron transfer process leads to the formation of the one-electron reduced tin chlorin π-radical anion $SnC^{\bullet-}$ as the first reaction intermediate (see eq 1).

$$SnC + D \xrightarrow{h\nu} D^{\bullet+} + SnC^{\bullet-} \quad (1)$$

In the case of similar sensitizers carrying high-valent main group central metals such as tin(IV) or antimony(V), it is well-established that such tetrapyrrole π-radical anions are metastable species,[50,63] which, under steady-state reaction conditions, are readily generated in degassed alkaline solution and identified by their weak Soret band at ~400 nm and a structured band pattern in the 700–800 nm spectral region (also see Figures 6 and 9). The chlorin π-radical anion $SnC^{\bullet-}$ can be reversibly further reduced in a second electron transfer step to generate the tin chlorin π-dianion species SnC^{2-} carrying two additional electrons in the aromatic ring system of the sensitizer. This process, which is considered as one of the crucial steps for coupling the initial one-electron photoreduction process to a net two-electron redox reactivity of the catalytic system, can proceed in two different ways. Depending on the sensitizer concentration and the nature of the electron donor D applied, a second electron transfer step (eq 2) or a disproportionation of the π-radical anion (eq 3) will finally lead to the formation of the diamagnetic SnC^{2-} dianion.

$$SnC^{\bullet-} + D^{\bullet+} \rightarrow D^{2+} + SnC^{2-} \quad (2)$$

$$2SnC^{\bullet-} \rightarrow SnC + SnC^{2-} \quad (3)$$

The π-dianion is able to take up one or two protons at different positions of the tetrapyrrole ring. These steps are critically influenced by pH, solvent, central atom, and substitution pattern of the macrocyclic system. The exact position of such a ring protonation can be clearly distinguished spectroscopically. In our case (Figures 9 and 10), the absence of a typical Soret band and the apparent bleaching of the entire spectrum of the sensitizer, leaving only broad, unstructured absorption bands in the 400–500 nm and 600–800 nm regions indicates the uptake of one additional proton in the *meso*-position of the macrocycle, thus forming a new compound with typical phlorin-anion characteristics.[50,64] A quite similar air-sensitive reduction

dx.doi.org/10.1021/ic401611v | *Inorg. Chem.* 2013, 52, 11910–11922

product of a metallochlorin has been described and characterized before by Stolzenberg and co-workers.[65]

$$SnC^{2-} + H^+ \rightarrow SnCH^- \quad (4)$$

The resulting tin(IV) chlorin-phlorin anion complex $SnCH^-$ containing a 2,3,10-saturated porphyrin ring chromophore (eq 4) is thought to be the mechanistic key intermediate acting as the photochemically produced primary hydride source for the further catalytic steps involved in NADH generation (see Figure 12).

Oxidation of $SnCH^-$ to completely regenerate the initial tin chlorin species may occur in the presence of dioxygen (Figure 10) or, much more importantly, by transferring two electrons and a proton to the rhodium co-catalyst to drive the reaction sequence given below (eqs 5 and 6). The net hydride transfer process described in eq 5 continuously recycles the photoreduced SnC sensitizer for further irradiation with red light, as already indicated in the simplified picture given in Scheme 2.

$$SnCH^- + [Cp^*Rh(bpy)H_2O]^{2+} \rightarrow H_2O + [Cp^*Rh(bpy)H]^+ + SnC \quad (5)$$

$$NAD^+ + [Cp^*Rh(bpy)H]^+ + H_2O \rightarrow [Cp^*Rh(bpy)H_2O]^{2+} + NADH \quad (6)$$

We have also shown, in different control experiments, that the chemically generated rhodium hydride complex $[Cp^*Rh(bpy)H]^+$ is able to reduce tin porphyrins to phlorin-type species in a proton-coupled two-electron transfer process related to the back reaction of eq 5, which additionally supports the possibility of a hydride exchange reaction sequence as proposed here (see the Supporting Information). It is also interesting to note that, during the course of all of the steady-state irradiation experiments reported here, an enhanced increase of NADH is always observed after a certain lag-phase, which is finished when the absorption spectrum of the chlorin-phlorin anion $SnCH^-$ is already dominating the photostationary mixture.

The suggested axial coordination sphere interaction between the reduced sensitizer $SnCH^-$ and the rhodium co-catalyst (Figure 12) is fully compatible with the well-established mechanism of regioselective 1,4-NADH formation based on mixtures of $[Cp^*Rh(bpy)H_2O]^{2+}$ and sacrificial hydride sources, which intermediately bind through an O-atom to the rhodium center.[40] Furthermore, the close proximity and face-to face alignment of the sensitizer and co-catalyst π-electron systems, as depicted in Figure 12, are expected to provide a very favorable situation[66] for effective electron transfer from the tetrapyrrole complex donor to the rhodium site acting as the two-electron acceptor.

It should be kept in mind, however, that only a detailed deuterium labeling study could provide direct evidence for this plausible but, at the moment, still tentative suggestion. It is also not yet clear whether a stepwise electron transfer sequence followed by protonation or a more or less concerted process is operating, although we assume that cleavage of the Rh−O bond and protonation of the Rh(I)-intermediate formed after two-electron reduction[39] is more probable.

In summary, the artificial photosynthetic NADH production described in the present work is thought to involve the photocatalytic formation of an intermediate hydride source (eq 7) coupled to a subsequent regioselective hydride transfer reaction (eq 8).

$$SnC + 2e^- + H^+ \xrightarrow{h\nu} SnCH^- \quad (7)$$

$$SnCH^- + NAD^+ \xrightarrow{cat} SnC + NADH \quad (8)$$

3. CONCLUSION

We have presented and characterized a new photocatalytic system for the regioselective two-electron reduction of nucleotide co-factors driven by light. For the first time, it could be demonstrated in an abiotic system that photons in the long-wavelength region of the visible spectrum (>610 nm) can be exploited to power the accumulation of NADH. Red-light energy could also be successfully converted using the synthetic co-factor analogue BNADH as a storage medium of reduction equivalents. The light-harvesting and photocatalytic product formation process was achieved with a tin(IV) chlorin complex (SnC), which showed an excellent water solubility and long-term stability. The artificial photosynthetic reaction sequence described here in detail, involving a primary electron donor, a multielectron transfer photosensitizer with a chlorophyll-type spectrum, and an additional redox-mediator catalyzing (B)NADH formation can be regarded as the first true functional model system for the overall light reactions occurring in natural photosystem I (PSI). It could be shown that various sacrificial donors, even in a very low excess, can be applied to maintain the energy-storing photoinduced electron transfer and chemical bond formation chain. More remarkably, the simple biomimetic process in an unprecedented way displays a very promising performance in terms of relevant efficiency criteria, including the limiting threshold energy of actinic light and the absolute quantum yield of permanent photoproduct formation. Both values are indeed approaching the orders of magnitude reported for natural photosynthesis. As part of our ongoing interest in bioinspired reaction cascades driven by sunlight and enzyme models,[2,13,67,68] we have also coupled an enzymatic dark reaction to the artificial photosynthesis of NADH. It turned out that, similar to the steady-state situation in natural photoautotrophic metabolism, such a consecutive reaction cascade helps to avoid back-reactions and other limitations caused by NADH instability, which, in our case, led to an approximately 10-fold improvement of the permanent product formation efficiency. Further mechanistic studies regarding the components of the photostationary reaction mixture and variations of the coupled substrate conversion routes based on photogenerated (B)NADH are currently underway.

4. EXPERIMENTAL SECTION

4.1. Materials and Instrumentation. All chemicals, if not otherwise stated, were used as supplied. Water was purified with a Milli-Q system (Millipore, Bedford, MA, USA). Absolute acetonitrile was added as an internal standard for the enzymatic reactions. Synthesis and characterization of the water-soluble tin-chlorin photosensitizer (SnC) and the nucleotide co-factor analogues $BNAD^+$ and BNADH are described in detail in the Supporting Information. The hydride transfer mediator precursor compound Cp*Rh(bpy)Cl]Cl was prepared following literature procedures.[69] Disodium ethylene diaminoacetate (Titriplex III) dihydrate salt p.a. (EDTA) was purchased from Merck and triethanolamine (98%) from ABCR Chemicals. Alcohol dehydrogenase (ADH) from *Saccharomyces cerevisiae* (≥300 units/mg protein) was purchased from Aldrich, as well as β-nicotine amide adenine dinucleotide hydrate from yeast (NAD^+).

dx.doi.org/10.1021/ic401611v | Inorg. Chem. 2013, 52, 11910−11922

For UV-vis-NIR absorption measurements up to 1100 nm, a Varian Cary 50 spectrophotometer was used. Luminescence spectra were recorded with a Horiba Jobin Yvon FluoroLog 3 modular spectrofluorometer equipped with two double-grating monochromators. Irradiation experiments were carried out on an optical bench in rectangular 1-cm quartz cuvettes. As the light source for polychromatic irradiation experiments, a 150 W xenon lamp (Osram, Model XBO 150W/1) was used with an Oriel Newport universal arc lamp housing equipped with an Aspherab UV-grade fused silica condenser lens and an AMKO IR liquid filter filled with water (80 mm light pass). The power supply was set to 100 W (5.6 A; 17.7 V) for all experiments. To cut off short-wavelength light, suitable Schott long-pass glass color filters were used: OG 530, OG 590 and RG 610, respectively. For the determination of quantum yields and for carrying out wavelength-selective irradiation experiments, different 3 W light-emitting diodes (LEDs) were used with λ_{max} = 525, 592, or 623 nm. All quantum yields were measured with a home-built setup calibrated against the ferrioxalate actinometer, as described in detail in the Supporting Information.

Room-temperature ^{1}H and ^{119}Sn NMR spectra were recorded on a Bruker DRX 500 spectrometer operating at 500.13 MHz (^{1}H) or at 186.4 MHz (^{119}Sn). Chemical shifts are either given in ppm, relative to residual solvent (H_2O 4.7 ppm) for ^{1}H, or were measured using $Sn(Ph)_4$ as a secondary standard for ^{119}Sn with all values reported relative to the external reference $Sn(Me)_4$ (δ = 0 ppm).

4.2. General Procedure for the Photoreduction of Nucleotide Co-factors. All photocatalytic experiments were performed at 298 K in 1-cm quartz cuvettes with screw caps and a septum. The samples were purged with nitrogen or argon, to remove most of the dioxygen from air, and were constantly stirred with a magnetic stirrer. Unless otherwise stated, a typical sample for an experiment had a volume of 3.2 mL, which consisted of an aqueous EDTA or TEOA solution (10 mM−1 M) with 0.1 M sodium phosphate buffer (pH 8.8 or 7.4). The catalyst concentrations were 7.5×10^{-6} M SnC and 7.7×10^{-5} M $[Cp^*Rh(bpy)H_2O]^{2+}$ (at pH 7.4) or $[Cp^*Rh(bpy)OH]^{+}$ (at pH 8.8), respectively. (B)NAD^+ (1 mM) was added to the solution, and the reaction progress was followed spectroscopically.

4.3. Catalytic Dark Reactions with NADH-Dependent Enzymes. Samples for coupling artificial photosynthetic NADH production to additional biochemical processes were prepared in 1-cm quartz cuvettes sealed with a septum and consisted of a 0.1 M EDTA solution in 0.1 M aqueous sodium phosphate buffer (pH 8.8). The photosensitizer and co-catalyst concentrations were 7.5 μM SnC and 7.7×10^{-5} M $[Cp^*Rh(bpy)OH]^{+}$, respectively. To the argon-purged solution (V = 3.2 mL), 2 mg of the NAD^+ co-factor (1 mM), 10 μL each of acetonitrile and butyraldehyde (35 mM), and 0.7 mg of lyophilized yeast alcohol dehydrogenase (ADH, Aldrich) were added. The sample was then irradiated under steady-state conditions with orange-red light (590 nm cutoff filter; 298 K). The reaction progress was followed and quantified by UV−vis spectroscopy and GC measurements.

■ ASSOCIATED CONTENT

Supporting Information

Details on the synthesis of the compounds used, as well as further spectroscopic and experimental data including more information on HPLC/HRMS analytics, photolysis experiments, and quantum yield determination procedures. This material is available free of charge via the Internet at http://pubs.acs.org.

■ AUTHOR INFORMATION

Corresponding Author

*E-mail: Guenther.Knoer@jku.at.

Notes

The authors declare no competing financial interest.

■ ACKNOWLEDGMENTS

We would like to thank Evren Aricanli for additional measurements. This manuscript is based on research supported by the Austrian Science Fund (FWF Project No. P21045, "Bio-inspired Multielectron Transfer Photosensitizers"). NMR facility funding from the European Union through the EFRE INTERREG IV ETC-AT-CZ program (Project No. M00146, "RERI-uasb") is gratefully acknowledged. G.K. also thanks the German Research Foundation (DFG No. GRK1626, "Chemical Photocatalysis") for partial support of this work.

■ ABBREVIATIONS

SnP = water-soluble tin(IV)-*meso*-tetrakis(*N*-methylpyridinium)-porphyrin complexes of the type $[(TMPyP)Sn(X)_2]^{4+}$ with X = Cl or OH, derived at different pH from the starting compound dichloro-(5,10,15,20-tetrakis(*N*-methylpyridinium-4-yl)-porphyrinato)tin(IV)-tetrachloride

SnC = water-soluble tin(IV)-*meso*-tetrakis(*N*-methylpyridinium)-chlorin complexes of the type $[(TMPyC)Sn(X)_2]^{4+}$ with X = Cl, or OH derived at different pH from dichloro-(2,3-dihydro-5,10,15,20-tetrakis(*N*-methylpyridinium-4-yl)-porphyrinato)tin(IV)-tetrachloride

$SnCH^-$ = Tin(IV)-*meso*-tetrakis(*N*-methylpyridinium)-chlorin-phlorin-anion complex of the type $[(TMPyCH)Sn(X)_2]^{3+}$ with X = Cl or OH, derived by monodeprotonation of dichloro-(2,3,10,23-tetrahydro-5,10,15,20-tetrakis(*N*-methylpyridinium-4-yl)-porphyrinato)tin(IV)-tetrachloride

NADH = 1,4-dihydro nicotine amide adenine dinucleotide

NAD^+ = nicotine amide adenine dinucleotide

BNADH = *N*-benzyl-1,4-dihydro nicotine amide

$BNAD^+$ = *N*-benzyl-3-carbamoyl-pyridinium cation

Chl = chlorophyll

D = sacrificial electron donor

$[Cp^*Rh(bpy)Cl]Cl$ = chloro-[η^5-(pentamethyl)-cyclopentadienyl]-(2,2′-bipyridyl)-rhodium(III) chloride

$[Cp^*Rh(bpy)H]^+$ = Hydrido-[η^5-(pentamethyl)-cyclopentadienyl]-(2,2′-bipyridyl)-rhodium(III) cation

ADH = alcohol dehydrogenase from *Saccharomyces cerevisiae*

EDTA = ethylenediamine-tetraacetic-acetate sodium salts

TEOA = triethanolamine

HPLC = high-performance liquid chromatography

HRMS = high-resolution mass spectrometry

ESI = electrospray ionization

GC = gas chromatography

NIR = near infrared

Q-TOF = quadrupole time-of-flight mass spectrometer

TON = turnover number

TOF = turnover frequency

U = unit of 1 μmol min^{-1} enzymatic activity

REFERENCES

(1) Bensaid, S.; Centi, G.; Garrone, E.; Perathoner, S.; Saracco, G. *ChemSusChem* **2012**, *5*, 500−521.
(2) Knör, G.; Monkowius, U. *Adv. Inorg. Chem.* **2011**, *63*, 235−289.
(3) Jensen, K.; Jensen, P. E.; Møller, B. L. *ACS Chem. Biol.* **2011**, *6*, 533−539.
(4) Lu, Y.; Zhang, C.; Zhao, H.; Xing, X.-H. *Appl. Biotechnol.* **2012**, *167*, 732−742.
(5) Obert, R.; Dave, B. C. *J. Am. Chem. Soc.* **1999**, *121*, 12192−12193.
(6) Chen, Q.-A.; Chen, M.-W.; Yu, C.-B.; Shi, L.; Wang, D.-S.; Yang, Y.; Zhou, Y.-G. *J. Am. Chem. Soc.* **2011**, *133*, 16432−16435.
(7) Berenguer-Murcia, A.; Fernandez-Lafuente, R. *Curr. Org. Chem.* **2010**, *14*, 1000−1021.
(8) Dibenedetto, A.; Stufano, P.; Macyk, W.; Fragale, C.; Costa, M.; Aresta, M. *ChemSusChem* **2012**, *5*, 373−378.
(9) Lee, S. H; Kim, J. H.; Park, C. B. *Chem.—Eur. J.* **2013**, *19*, 4392−4406.
(10) Hollmann, F.; Arends, I. W. C. E.; Buehler, K. *ChemCatChem* **2010**, *2*, 762−782.
(11) Portenkirchner, E.; Oppelt, K. T.; Egbe, D. A. M.; Knör, G.; Sariciftci, N. S. *Nanomater. Energy* **2013**, *2*, 134−147.
(12) Buchler, J. W. In *The Porphyrins, Vol. I*; Dolphin, D., Ed.; Academic Press: New York, 1978; p 390.
(13) Knör, G. *Coord. Chem. Rev.* **1998**, *171*, 61−70.
(14) Arnold, D. P.; Blok, J. *Coord. Chem. Rev.* **2004**, *248*, 299−319.
(15) Krüger, W.; Fuhrhop, J.-H. *Angew. Chem.* **1982**, *94*, 132−133.
(16) Handman, J.; Harriman, A.; Porter, G. *Nature* **1984**, *307*, 534−535.
(17) Whitten, D. G.; Yau, J. C. N.; Carroll, F. *J. Am. Chem. Soc.* **1971**, *93*, 2291−2296.
(18) Harriman, A. *J. Photochem.* **1985**, *29*, 139−150.
(19) Kalyanasundaram, K. *Photochemistry of Polypyridine and Porphyrin Complexes*; Academic Press: London, 1992; p 462 ff.
(20) Hawley, J. C.; Bampos, N.; Abraham, R. J.; Sanders, J. K. M. *Chem. Commun.* **1998**, 661−662.
(21) Takagi, S.; Morimoto, H.; Shiragami, T.; Inoue, H. *Res. Chem. Intermed.* **2000**, *26*, 171−183.
(22) Indelli, M. T.; Chiorboli, C.; Ghirotti, M.; Orlandi, M.; Scandola, F.; Kim, H. J.; Kim, H.-J *J. Phys. Chem. B* **2010**, *114*, 14273−14282.
(23) Lazarides, T.; Kuhri, S.; Charalambidis, G.; Panda, M. K.; Guldi, D. M.; Coutsoulelos, A. G. *Inorg. Chem.* **2012**, *51*, 4193−4204.
(24) Shetty, V. S.; Yogita, P.; Ravikanth, M. *Coord. Chem. Rev.* **2012**, *256*, 2816−2842.
(25) Harriman, A.; Walters, P. *Inorg. Chim. Acta* **1984**, *83*, 151−154.
(26) Harriman, A.; Porter, G.; Walters, P. *J. Chem. Soc., Faraday Trans. 1* **1983**, *79*, 1335−1350.
(27) Crossley, M. J.; Thordarson, P.; Wu, R. A.-S. *J. Chem. Soc., Perkin Trans. 1* **2001**, 2294−2302.
(28) Shetti, V. S.; Ravikanth, M. *J. Porph. Phthaloc.* **2010**, *14*, 361−370.
(29) Qu, Z.; Wenbo, E.; Zhu, W.; Thordarson, P.; Sintic, P. J.; Crossley, M. J.; Kadish, K. M. *Inorg. Chem.* **2007**, *46*, 10840−10849.
(30) Arnold, D. P.; Bartley, J. P. *Inorg. Chem.* **1994**, *33*, 1486−1490.
(31) Medforth, C. J. In *The Porphyrin Handbook*, Vol. *5*; Kadish, K. M., Smith, K. M., Guilard, R., Eds.; Academic Press: London, 2000; Chapter 35.
(32) Knör, G.; Vogler, A. *Inorg. Chem.* **1994**, *33*, 314−318.
(33) Lomova, T. N.; Tulaeva, E. Y.; Mozhzhukhina, E. G.; Klyueva, M. E. *Mendeleev Commun.* **1997**, *7*, 225−227.
(34) Delmarre, D.; Veret-Lemarinier, A.-V.; Bied-Charreton, C. *J. Luminesc.* **1999**, *82*, 57−67.
(35) Seely, G. R. *J. Chem. Phys.* **1957**, *27*, 125−133.
(36) Debaig-Valade, C.; Bagno, O.; Pommier, J. C.; Joussot-Dubien, J. *Photochem. Photobiol.* **1981**, *33*, 899−902.
(37) Scheer, H., Ed. *Chlorophylls*; CRC Press: Boca Raton, FL, 1991.
(38) Chen, M.; Scheer, H. *J. Porph. Phthaloc.* **2013**, *17*, 1−15.
(39) Steckhan, E.; Herrmann, S.; Ruppert, R.; Dietz, E.; Frede, M.; Spika, E. *Organometallics* **1991**, *10*, 1568−1577. Dadci, L.; Elias, H.; Frey, U.; Hörning, A.; Kölle, U.; Merbach, A. E.; Paulus, H.; Schneider, J. S. *Inorg. Chem.* **1995**, *34*, 306−315.
(40) Lo, H. C.; Leiva, C.; Buriez, O.; Kerr, J. B.; Olmstead, M. M.; Fish, R. H. *Inorg. Chem.* **2001**, *40*, 6705−6716.
(41) Lee, S. H.; Ryu, J.; Nam, D. H.; Park, C. B. *Chem. Commun.* **2011**, *47*, 4643−4645.
(42) Nam, D. H.; Park, C. B. *ChemBioChem* **2012**, *13*, 1278−1282.
(43) Liu, J.; Antonietti, M. *Energy Environ. Sci.* **2013**, *6*, 1486−1493.
(44) Karrer, P.; Schwarzenbach, G.; Benz, F.; Solmssen, U. *Helv. Chim. Acta* **1936**, *19*, 811−828.
(45) Bisswanger, H. *Practical Enzymology*, 2nd ed.; Wiley−VCH; Weinheim, Germany, 2011.
(46) The TON value is given here for a situation where the catalyst is still completely active and also the product accumulation is not yet levelling off to reach an absolute maximum. Therefore it clearly indicates that the process is non-stoiciometric, but should not be misunderstood as an upper limit of performance. For a critical discussion of current definitions and limitations using TON values, see: Kozuch, S.; Martin, J. M. L. *ACS Catal.* **2012**, *2*, 2787.
(47) Nucleotide co-factor regeneration is a net two-electron process, which may require the subsequent absorption of two photons per product molecule depending on the actual reaction mechanism. Some groups therefore calculate their quantum yield values as (2 × moles of product generated) per mole of incident photons. In our case, this would then double all of the reported quantum yield, TOF, and TON data.
(48) Matsubara, Y.; Koga, K.; Kobayashi, A.; Konno, H.; Sakamoto, K.; Morimoto, T.; Ishitani, O. *J. Am. Chem. Soc.* **2010**, *132*, 10547−10552.
(49) Kobayashi, A.; Takatori, R.; Kikuchi, I.; Konno, H.; Sakamoto, K.; Ishitani, O. *Organometallics* **2001**, *20*, 3361−3363.
(50) Baral, S.; Hambright, P.; Neta, P. *J. Phys. Chem.* **1984**, *88*, 1595−1600.
(51) Assuming that EDTA acts as a sacrificial one-electron donor, there is only a 5-fold excess of reductant available for the photocatalytic NADH production under these conditions.
(52) Note that TOF values are usually increasing with the incident light intensity in such systems, which is determined by the experimental setup used. Therefore, only quantum yield data are meaningful parameters for comparing the absolute performance of different photocatalysts at a certain excitation wavelength.
(53) Oren, A.; Padan, E.; Avron, M. *Proc. Natl. Acad. Sci. U.S.A.* **1977**, *74*, 2152−2156.
(54) Barber, J.; Melis, A. *Biochim. Biophys. Acta* **1990**, *1020*, 285−289.
(55) Terashima, I.; Fujita, T.; Inoue, T.; Chow, W. S.; Oguchi, R. *Plant Cell. Physol.* **2009**, *60*, 684−697.
(56) Oppenheimer, N. J.; Kaplan, N. O. *Biochemistry* **1974**, *13*, 4675−4685.
(57) Leskovac, V.; Trivić, S.; Peričin, D. *FEMS Yeast Res.* **2002**, *2*, 481−494.
(58) Mandler, D.; Willner, I. *J. Chem. Soc., Perkin Trans. 2* **1986**, 805−811.
(59) Lo, H. C.; Fish, R. H. *Angew. Chem., Int. Ed.* **2002**, *41*, 478−481.
(60) Green, D. W.; Sun, H. W.; Plapp, B. V. *J. Biol. Chem.* **1993**, *268*, 7792−7798.
(61) Rumeau, D.; Peltier, G.; Cournac, L. *Plant Cell. Environ.* **2007**, *30*, 1041−1051.
(62) Iwai, M.; Takizawa, K.; Tokutsu, R.; Okamuro, A.; Takahashi, Y.; Minagawa, J. *Nature* **2010**, *464*, 1210−1214.
(63) Knör, G.; Vogler, A.; Roffia, S.; Paolucci, F.; Balzani, V. *Chem. Commun.* **1996**, 1643−1644.
(64) Chirvony, V. S.; Sinyakov, G. N.; Gadonas, I. L.; Krasauskas, V.; Pelakauskas, A. *SPIE Laser Applications in Life Sciences* **1990**, *1403*, 504−506.
(65) Stolzenberg, A. M.; Stershic, M. T. *J. Am. Chem. Soc.* **1988**, *110*, 6391−6402.

(66) Ciammaichella, A.; Dral, P. O.; Clark, T.; Tagliatesta, P.; Sekita, M.; Guldi, D. M. *Chem.—Eur. J.* **2012**, *18*, 14008−14016.
(67) Hajimohammadi, M.; Schwarzinger, C.; Knör, G. *RSC Adv.* **2012**, *2*, 3257−3260.
(68) For a discussion on artificial photoenzymes, see: Stochel, G., Brindell, M., Macyk, W., Stasicka, Z., Szaciłowski, K., Eds. *Bioinorganic Photochemistry*; Wiley: Chichester, U.K., 2009; p 197.
(69) Kölle, U.; Grätzel, M. *Angew. Chem.* **1987**, *99*, 572−574.